

# UC San Diego

## UC San Diego Electronic Theses and Dissertations

### Title

Characterization of Myosin Phosphatase Targeting Subunit 2 Knockout Mice

### Permalink

<https://escholarship.org/uc/item/2cz006h1>

### Author

Hu, Tingfei

### Publication Date

2021

Peer reviewed|Thesis/dissertation

UNIVERSITY OF CALIFORNIA SAN DIEGO

Characterization of Myosin Phosphatase Targeting Subunit 2 Knockout Mice

A Thesis submitted in partial satisfaction of the requirements for the degree Master of Science

in

Biology

by

Tingfei Hu

Committee in charge:

Professor Renate B. Pilz, Chair

Professor Julian Schroeder, Co-Chair

Professor Katherine Petrie

2021

Copyright  
Tingfei Hu, 2021  
All rights reserved.

The Thesis of Tingfei Hu is approved, and it is acceptable in quality and form for publication on microfilm and electronically.

University of California San Diego

2021

## DEDICATION

I would like to dedicate this to my family for always supporting me and enabling me to pursue my interests.

## TABLE OF CONTENTS

Thesis Approval Page .....	iii
Dedication .....	iv
Table of Contents .....	v
List of Figures .....	vi
Acknowledgements .....	vii
Abstract of the Thesis .....	viii
Introduction .....	1
Materials and Methods .....	7
Results .....	11
Discussion .....	23
References .....	25

## LIST OF FIGURES

Figure 1. Quaternary Structure of Muscle Myosin .....	2
Figure 2. Schematic Representation of Myosin Phosphatase Complex.....	6
Figure 3. Identification of MYPT2 Knockout Mice .....	12
Figure 4. Antibody Test .....	14
Figure 5. Morphometric Measurements .....	16
Figure 6. Echocardiogram Measurements .....	18
Figure 7. Alterations in Hypertrophic Molecular Markers.....	22

## ACKNOWLEDGEMENTS

I would like to first thank Dr. Renate B. Pilz and Dr. Gerry R. Boss for the opportunity to join the lab and be part of their team. Under Dr. Renate B. Pilz's guidance the past few years, I have gained valuable insights and advice ranging from laboratory related subject matter to plausible career paths. I would also like to thank Dr. Darren Casteel for mentoring me the past few years and guiding me to become a better researcher. I would not have been able to grow in my research without his dedication to teaching and mentoring.

I would also like to thank Dr. Julian Schroeder and Dr. Katherine Petrie for being my committee members.

Finally, I am grateful to Dr. Renate B. Pilz and Darren Casteel for their editorial advice of my written thesis and PowerPoint presentation; additionally, I would like to thank members of the Boss-Pilz Laboratory for their helpful advice and discussion points.

Results are currently being prepared for submission for publication of the material. Pilz, Renate; Hu, Tingfei; and Casteel, Darren. The thesis author will be co-author of this material.

## ABSTRACT OF THE THESIS

Characterization of Myosin Phosphatase Targeting Subunit 2 Knockout Mice

by

Tingfei Hu

Master of Science in Biology

University of California San Diego, 2021

Professor Renate B. Pilz, Chair  
Professor Julian Schroeder, Co- Chair

Proper cardiac contraction is vital to maintain cardiovascular health and is modulated by the phosphorylation state of myosin regulatory light chain (MLC). The extent of MLC phosphorylation is dependent on the activities of both MLC kinase and MLC phosphatase. One prominent MLC phosphatase subunit found in cardiac muscle is Myosin Phosphatase Targeting

Subunit 2 (MYPT2). It was previously shown that an overexpression of MYPT2 resulted in a decreased level of MLC phosphorylation, resulting in reduction of left ventricular contraction and induction of hypertrophy. However, no studies have examined the effect of knocking out MYPT2 in mice. Therefore, we obtained heterozygous mice, containing a MYPT2 null allele from the Mutant Mouse Resource Center, to examine their phenotype and signaling pathways involved in cardiac cell growth. Phenotypically, we observed that MYPT2 knockout mice had decreased heart size and weight, with increased fractional shortening, as assessed by cardiac echogram. For the signaling pathways, we found no alteration in AKT or ERK signaling using western blot analysis; however, qPCR analysis showed that MYPT2 knockout showed an upregulation of atrial natriuretic peptide and downregulation  $\beta$ -myosin heavy chain transcripts. These studies provide evidence for the critical role that MYPT2 plays in normal cardiac function.

## **Introduction**

### **1.1 Striated Muscle Contraction Overview**

The sarcomere is the basic contractile unit in myocytes (1). An individual sarcomere is composed of both thin and thick filaments that slide past each other during muscle contraction and relaxation. The thin filament consists of two intertwined chains of actin with regulatory proteins troponin and tropomyosin, whereas the thick filament consists of organized bundles of myosin. When an electrochemical signal propagates down a myocyte,  $\text{Ca}^{2+}$  diffuses out of the sarcoplasmic reticulum and is bound to troponin. The transient attachment of  $\text{Ca}^{2+}$  to troponin exposes the myosin-binding sites on the actin filament, positioning myosin to its *on* conformation. This orientation enables the attachment of myosin head to the myosin-binding site, forming the actin-myosin crossbridge. The formation of the crossbridge permits muscle contraction as myosin pulls actin towards the M-line of the sarcomere. Following muscle contraction is muscle relaxation. When the electrochemical signal stops,  $\text{Ca}^{2+}$  is actively pumped back into the sarcoplasmic reticulum, detaching actin from myosin, and enabling another cycle of muscle contraction.

### **1.2 Structure of Myosin**

One functional unit of myosin contains both the myosin light chains (MLC) and myosin heavy chains (MHC) (2). The two major types of MLCs are the essential and the regulatory MLC. The three different subdomains of MHC are the coiled coil domain which mediates dimerization of two heavy chains, a lever arm with binding sites for MLC, and a head domain which forms actin-myosin cross bridges (Figure 1). The phosphorylation state of the regulatory MLC modulates the binding of the MHC head to actin, permitting muscle contraction and relaxation (3,4).

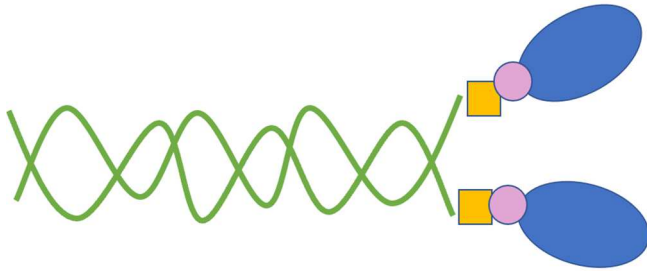


**Figure 1. Quaternary Structure of Muscle Myosin:** Myosin is a motor protein composed of two heavy chains, two essential light chains, and two regulatory light chains. The heavy chain heads are shown in blue; the heavy chain tail is shown in green. The essential light chains are shown in pink, and the regulatory light chains are shown in orange.

### **1.3 Posttranslational Modification of Myosin**

Cardiac muscle contraction is influenced by varying posttranslational modifications of both thick and thin filaments. In this study, we focus on the phosphorylation of regulatory MLC, which is part of the thick filament.

When the MLC of cardiac striated muscle is phosphorylated, contraction is not directly initiated but rather modulated. Contraction is directly initiated by  $\text{Ca}^{2+}$ , which exposes the myosin binding site on actin and enables the attachment of MHC head, leading to actin-myosin power stroke. The phosphorylation state of MLC modulates cardiac contraction by altering the efficiency of MHC head and actin interaction (3). Phosphorylated MLC increases the efficiency of actin-myosin binding by orienting the MHC head perpendicular to actin; de-phosphorylated MLC decreases the efficiency of actin-myosin binding by reorienting the MLC head parallel to actin.

### **1.4 Myosin Light Chain Phosphatase**

The phosphorylation status of MLC is dependent on both the MLC kinases and MLC phosphatases. However, MLC kinases and MLC phosphatases of cardiac muscles have not been well characterized. MLC phosphatases are heterotrimers, composed of three unique subunits (5). It contains PP1c $\delta$  (a catalytic subunit), a small subunit (M20) of relatively unknown function, and a myosin binding subunit (MYPT) which contains binding sites for PP1c $\delta$ , myosin, and M20 (Figure 2).

The diversity of MLC phosphatases is owed to the varying MYPT subunits, which include MYPT1, MYPT2, MBS85, MYPT3, and TIMAP (6). The identity of the MYPT is dependent on the tissue type. The prominent regulatory phosphatase subunits we focus on for this study are MYPT1 (115-kDa) and MBS85 (85-kDa) for smooth muscles and MYPT2 (110-

kDa) for striated cardiac muscles. These three MYPT are the product of different genes. The MYPT1 gene is located on chromosome 12q15 – q21.2; the MYPT2 gene is located on chromosome 1q32.1; and the MBS85 gene is located on 19q13.42. When amino acid sequences are compared to MYPT1, the overall sequence similarities are 61% for MYPT2 and 39% for MBS85. The binding of MYPT family proteins to PP1c $\delta$  targets MLC phosphatase to region specific myosin, such as those in smooth and striated muscles. MYPT also regulates PP1c $\delta$  catalytic activity. Binding of the MYPT N-terminus to PP1c $\delta$  increases PP1c $\delta$  phosphatase activity (7,8); however, phosphorylation of residues in the MYPT C-terminus (by ROCK or other kinases), leads to inhibition of catalytic activity (9-12). The phosphorylated MYPT residue is located in a structural loop that binds to the PP1c $\delta$  catalytic site and blocks MLC access (13).

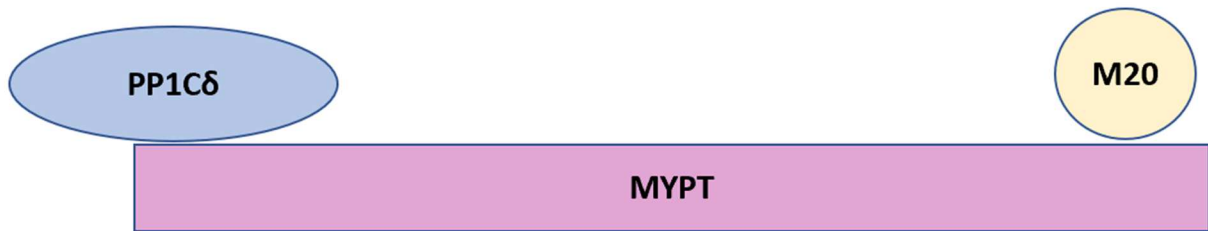


**Figure 2. Schematic Representation of Myosin Phosphatase Complex.**

The PP1C $\delta$  binding domain is shown in blue, the M20 is shown in yellow, and the myosin phosphatase regulatory subunit is shown in pink.

## **1.5 Smooth and Striated Muscle Relaxation and Contraction**

Both smooth and striated muscles contain MLC phosphatase that is composed of PP1c $\delta$ , MYPT, and M20. The binding of MYPT to PP1c $\delta$  enhances the hydrolysis activity of PP1c $\delta$  on the phosphate of either the serine or threonine residues of MLC, resulting in effects that depend on the tissue type and identity of the MYPT subunit. De-phosphorylation of MLC by the MYPT1-containing complex, predominantly found in smooth muscle cells, directly drives relaxation and regulates vascular tone (14); whereas de-phosphorylation of MLC by the MYPT2-containing complex in striated muscle cells, only modulates muscle relaxation. In cardiac myocytes, the cycle of contraction and relaxation is mainly driven by Ca<sup>2+</sup> levels.

## **1.6 Characterization of Mice Overexpressing MYPT2**

Transgenic mice (Tg) with cardiac specific MYPT2 overexpression showed a decrease in the amount of phosphorylated MLC (14). These Tg mice appeared and behaved normally when compared to wild-type mice. However, it was found that cardiac specific overexpression of MYPT2 led to hypertrophic cardiomyopathy, and that the degree of hypertrophy correlated with the extent of MYPT2 overexpression. H&E staining of heart tissue showed that overexpression of MYPT2 led to an increase in left ventricular dimensions and an increase in heart to body weight ratio, indicating an enlargement of the heart. Overexpression of MYPT2 also led to increased expression of brain natriuretic peptide and  $\beta$ -myosin heavy chain, which are molecular markers for hypertrophy. The mice showed an increase in the end-systolic and end-diastolic volumes due to reduced fractional shortening. Since my project is focused on MYPT2 knockout mice, we expect to see the opposite phenotypic findings when we characterize MYPT2 knockout mice.

## Materials and Methods

### 2.1 Materials

MYPT2 knockout mice were produced by the Mutant Mouse Resource Center and obtained from Jackson laboratory (MMRRC Stock No: 46179-JAX). Dulbecco's Modified Eagle Medium (DMEM) was from Cellgro. Fetal bovine serum (FBS) was from Sigma-Aldrich. Restriction enzymes were from New England Biolabs. Protease inhibitor cocktail was from EMD Millipore Corporation (Cat#: 539131). Anti-Flag antibody was from Sigma-Aldrich. Rabbit anti-MYPT1/2 was from Abcam (Cat#: ab32519). Anti-PP1c $\delta$  antibody was from Origene (Cat#: TA308937). HRP conjugated anti- $\beta$ -actin antibody was from Santa Cruz Biotechnology (Cat#: sc-47778-HRP). Peroxidase-conjugated Goat anti-Rabbit IgG was from Jackson ImmunoResearch (Cat#: 111-035-003). SuperSignal West Pico Plus was from Pierce (Cat#: 34580). IRDye 680RD Goat anti-mouse and IR DYE 800CW Goat anti-Rabbit, and Intercept Blocking Buffer were from LI-COR. Other general chemicals and supplies were from Fisher Scientific or Sigma-Aldrich.

### 2.2 Cell culture

293T cells were grown in Dulbecco's Modified Eagle Medium DMEM (Cellgro) with 10% fetal calf serum (Sigma-Aldrich) at 37°C with 5% CO<sub>2</sub> in a water jacketed incubator. Stock cells were grown in 10 cm tissue culture dishes and cells were split every two to three days using 0.25% trypsin/EDTA (Gibco).

### 2.3 MYPT2 Knockout Mice

All animal experiments were approved by the Institutional Care and Use Committee of the University of California, San Diego. 12 or 25 weeks old Mice were used (C57BL/6NJ-*Ppp1r12b*<sup>em1(IMPC)*J*</sup>/Mmjax) to generate data. They were housed in a temperature-controlled

environment with a 12/12 h light/dark cycle. Mice were weaned at day 18, and genotyped by polymerase chain reaction (PCR) and agarose gel electrophoresis using genomic DNA from approximately 2 mm of clipped mouse tail. The genomic DNA was obtained by incubation of the tail in 75 $\mu$ L of 25mM NaOH/0.2mM EDTA at 98°C for 1h. The tube was then cooled to room temperature before 75 $\mu$ L of 40mM tris HCl (pH 5.5) was added. Sample was next vortexed and 1  $\mu$ L was aliquoted for PCR. The PCR reaction was run using HotStart Taq polymerase (BioPioneer, catalog #: MAT-4) along with the following primers: 5'-TGTTTTCCCTACTTGCTGTG-3' and 5'-GCTTGTGTTCTGCTGTTT-3'. The wild-type gene product was 775 bp and the mutant gene product was 195 bp.

#### **2.4 Expression Vectors and Transfection**

The expression vectors of MYPT1, MYPT2, and MBS85 were engineered with N-terminal FLAG tags. They were then transfected into 293T cells using Lipofectamine<sup>2000</sup> (ThermoFisher). For each transfected sample, DNA/Opti-MEM and Lipofectamine<sup>2000</sup>/Opti-MEM mixtures were incubated for 5-minute at room temperature. The two incubations were mixed and incubated for an additional 20 min at room temperature. The mixtures were then added to 293T cells and kept at 37°C for 24 h before harvesting.

#### **2.5 Western blot**

For transfected 293T cells, lysates were prepared by aspirating the media from the cells and directly scraping in ice cold Lysis Buffer 1 (phosphate buffered saline, 0.1% NP40 and protease inhibitor cocktail). Lysates were cleared by centrifugation at 16,000g for 10 minutes at 4° C, and cleared lysates were mixed 2:1 in 3x in sodium dodecyl sulfate sample (SDS) sample buffer. Equal amounts of lysates were separated by SDS-polyacrylamide gel electrophoresis (PAGE).

For transgenic MYPT2 knockout mice, frozen tissues were pulverized, resuspended in 1x SDS sample buffer, and sonicated 2x 20 seconds on ice. Proteins were quantified using a Bradford assay, and 80 µg protein from each tissue were separated by SDS-PAGE.

Proteins were transferred to Polyvinylidene difluoride (PVDF) membrane and blocked in 5% milk in Tris-buffered saline (TBS). For blots using infrared dye (IR Dye) secondary antibodies, proteins were transferred to Immobilon-FL PVDF membrane and blocked in Intercept Blocking Buffer (LI-COR).

Western blots were performed with antibodies directed against Flag-epitope (1:5000), MYPT1/2/MBS85 (1:2000), PP1Cδ (1:2000) and HRP-conjugated β-actin (1:10,000). HRP-conjugated secondary antibodies were used at 1:5000 and IR-dye secondary antibodies were used at 1:10,000. Antibodies were diluted in the blocking buffer used for each condition. HRP blots were visualized using SuperSignal West Pico Plus chemiluminescent western blotting substrate and IR blots were visualized using an Odyssey Imaging System (LI-COR).

## **2.6 Quantitative RT-PCR**

Within five minutes of euthanasia of MYPT2 knockout mice, hearts were snap-frozen in liquid nitrogen then pulverized and resuspended in Trizol (Molecular Res.Center, TR118). Total RNA was isolated as per the manufacturer's instructions. Total RNA was reverse-transcribed using iScript cDNA synthesis kit (Bio-Rad). Quantitative PCR was performed using a MX3005P real-time PCR detection system with Brilliant II SYBR Green Mix (Agilent Technologies) as described. All primers were intron-spanning and were tested with serial cDNA dilutions. Relative changes in mRNA expression were analyzed using the comparative  $2^{-\Delta\Delta C_t}$  method.

## **2.7 Echocardiography**

To perform echocardiography, 24-week-old male mice had their chest hair removed using Nair hair removal lotion. Mice were anesthetized with 5% isoflurane and maintained on 0.5% isoflurane. Electrocardiograms were monitored with probes inserted into the upper and lower torso. Cardiac function was recorded with a VisualSonics, SonoSite FUJIFILM, Vevo 2100 ultrasound system with a linear transducer 32–55 MHz by a single, highly experienced operator who was blinded to the genotype of the mice.

## **2.8 Statistical Analysis**

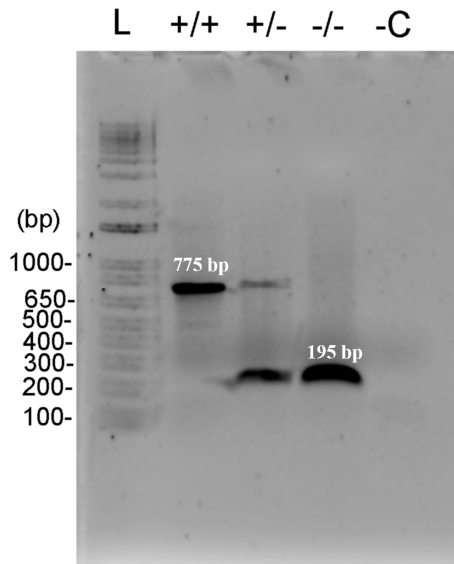
Data are reported as mean  $\pm$  standard deviation. Comparisons between groups were performed by two-tailed Student's T-Test. A value of  $p < 0.05$  was considered statistically significant.

## Results

### 3.1 Homozygous MYPT2 Knockout Mice are Viable

It was previously shown that global homozygous MYPT1 knockout mice are not viable (15). Whether global homozygous MYPT2 knockout mice would be non-viable as well is unknown. We obtained male and female heterozygous MYPT2 knockout mice from the Jackson laboratory, generated with the CRISPR/Cas9 technology by the Mutant Mouse Resource Center, and set up breeding between them. We found that homozygous MYPT2 knockout mice were born and viable as determined by genotyping at the time of weaning (Figure 3A). The knockout mice were kept to at least 24-weeks of age, and they appeared normal and showed no obvious health or behavioral issues when compared to wild-type mice. To examine MYPT expression, we used heart lysates from 24-week-old mice and performed Western blot using MYPT1/2 antibodies. As seen in Figure 3B, MYPT2 expression was lower in heterozygous mice and absent in the homozygous knockout mice. Expression of catalytic PP1C $\delta$  subunit also decreased when MYPT2 expression was decreased. MYPT1 expression was much lower than MYPT2 expression and remained relatively constant throughout the three genotypes, suggesting no apparent compensatory upregulation of MYPT1. There was no MBS85 expression detected in the heart lysates.

**A**



**B**

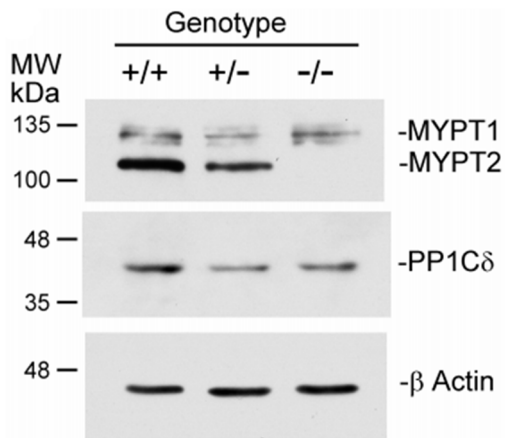
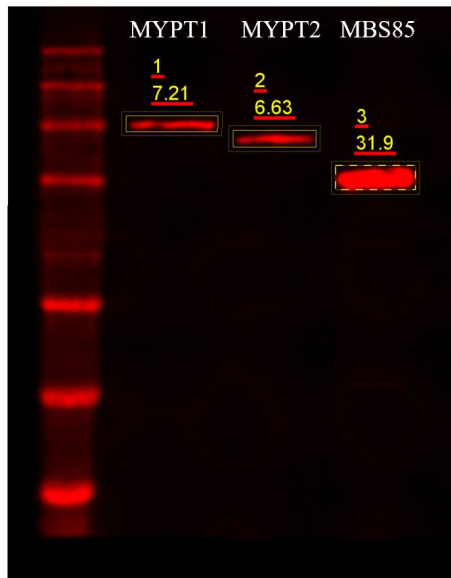


**Figure 3. Identification of MYPT2 Knockout Mice.** (A) Agarose gel electrophoresis of MYPT2 genotyping PCR products in wild-type (+/+), heterozygous (+/-), and homozygous (-/-) mice. The wild-type allele produced a 775 base pair product, and the mutant allele produced a 195 base pair product. (B) Western blots of heart lysates from 24-week-old mice for myosin regulatory subunits and PP1Cδ for +/+, +/-, and -/- mice.

### 3.2 MYPT1/2 Antibody Test

MYPT1, MYPT2, and MBS85 are homologues of each other, with MYPT1 and MYPT2 being closely related and MBS85 being more distant. Since these proteins have similar amino acid sequences, we used a commercially available antibody known to cross-recognize MYPT1 and MYPT2. However, its recognition of MBS85 and its sensitivity to each protein are unknown. To assess the antibody's specificity and sensitivity, we transfected 293T cells with Flag-tagged expression vectors for MYPT1, MYPT2, and MBS85. The cell lysates were then analyzed by Western blot and probed with an anti-Flag antibody followed by an infra-red IR-Dye 680RD secondary antibody. Imaging was done using a LI-COR Odyssey Fc system. As seen in Figure 3B, the expression of MYPT1 and MYPT2 were similar, and the expression of MBS85 was ~5-fold higher. Probing the same membrane with the anti-MYPT1/2 antibody followed by an IR-Dye 800CW secondary, we again observe similar expression levels of MYPT1 and MYPT2 (Figure 4B). Interestingly, the apparent MBS85 signal was only ~1.4-fold higher than that of MYPT1/2, indicating that the antibody was less sensitive toward MBS85.

A



B



**Figure 4. Antibody Test.** (A) Cell lysates from 293T cells expressing Flag-tagged MYPT1, MYPT2, or MBS85 were probed with mouse anti-Flag antibody followed by an IR Dye 680RD antibody. Protein expression levels were quantified using a LI-COR Odyssey imaging system. (B) The same blot, as shown in A, was probed with rabbit anti-MYPT1/2 antibody followed by an IR Dye 800CW antibody. Proteins were quantified as described for A.

### **3.3 Body and Tissue Weights**

Since global MYPT2 knockout mice have yet to be characterized, we assessed whether knocking out MYPT2 has a general effect on the body and tissue weights. The body weights were not significantly different between wild-type, heterozygous, or homozygous mice (Figure 5A). The heart weight to body weight ratio was significantly decreased in the knockout mice (Figure 4B) while the kidney to body weight ratio was similar in all three genotypes (Figure 4C). The lung to body weight ratio was lower in the heterozygous compared to wild-type but did not differ between the wild-type and knock out mice (Figure 4D). The result seen in Figure 4D may be due the small sample size and the presence of an outlier mouse. Overall, these results showed that MYPT2 knockout mice exhibited lighter hearts.

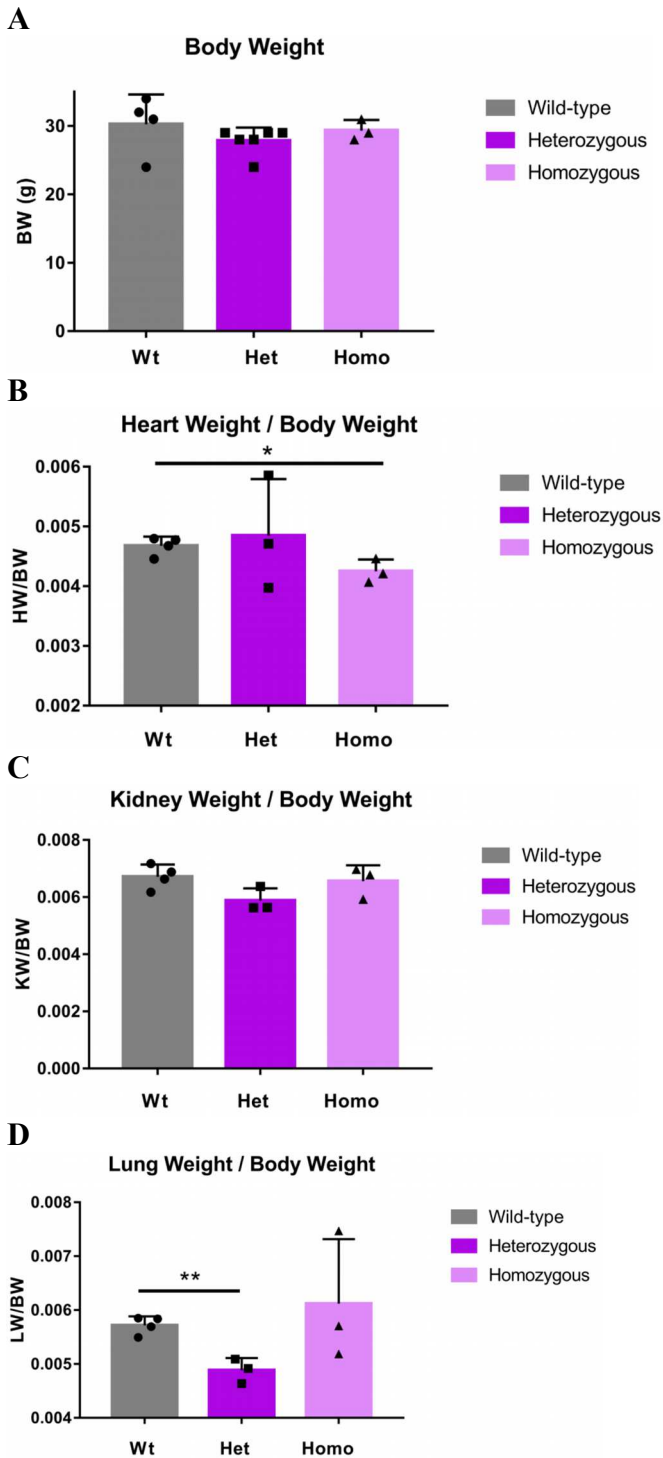


**Figure 5. Morphometric Measurements.** (A -D) Values reported are mean  $\pm$  standard deviation. \* indicates a value of  $p < 0.05$ . \*\* indicates a value of  $p < 0.01$ . BW, body weight; HW, heart weight; KW, kidney weight; LW, lung weight.

### **3.4 Changes in Cardiac Morphology and Function**

Since MYPT2 is believed to play a critical role in cardiac physiology, we used echocardiography to examine the effect of MYPT2 deletion on cardiac size and function. As shown in Figure 6A, fractional shortening increased for homozygous knockout mice when compared to wild-type mice. This increase in contractility is inversely proportional to the left ventricular mass to body weight ratio (Figure 5B) and the left internal diameter at the end of diastole to body weight ratio (Figure 5C). Both ratios were significantly lower for homozygous than heterozygous, indicating a decrease in cardiac size. This result is consistent with the smaller heart weights shown in Figure 4B.

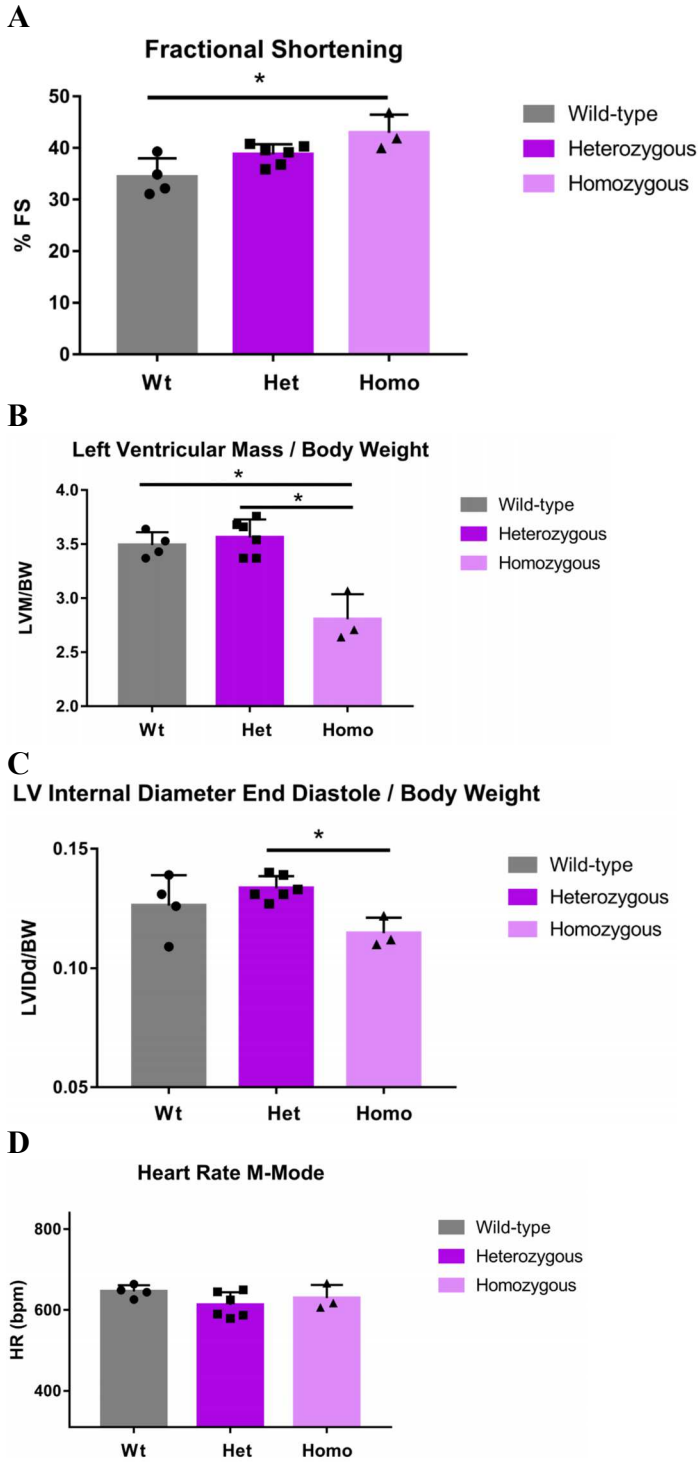


**Figure 6. Echocardiogram Measurements.** (A - D) Values reported are mean  $\pm$  standard deviation. \* indicates a value of  $p < 0.05$ . FS, fractional shortening; LVM, left ventricular mass; LV, left ventricular; BW, body weight; LVIDd, left ventricular internal diameter end diastole.

### **3.5 Examination of the AKT and ERK signaling pathways**

During stress that drives cardiac hypertrophy, the AKT and ERK cell growth pathways are activated (16). Specifically, both phosphorylated AKT and ERK levels increase under cardiac hypertrophic conditions. Since overexpression of MYPT2 is linked with hypertrophy (14), we explored the link between hypertrophic pathways and the smaller heart size as seen in our mice. Given that MYPT2 knockout mice had smaller hearts, we reasoned that growth promoting pathways would be downregulated and expected to observe lower basal AKT and ERK phosphorylation levels. However, using Western blotting, we found no consistent change in the phosphorylation levels of these two proteins (Figure 6).

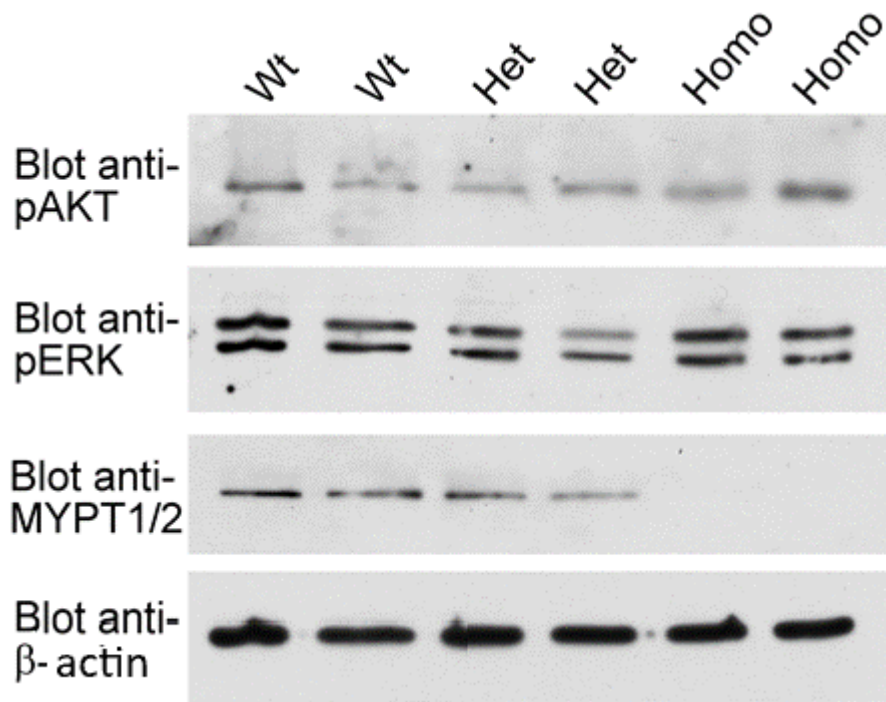


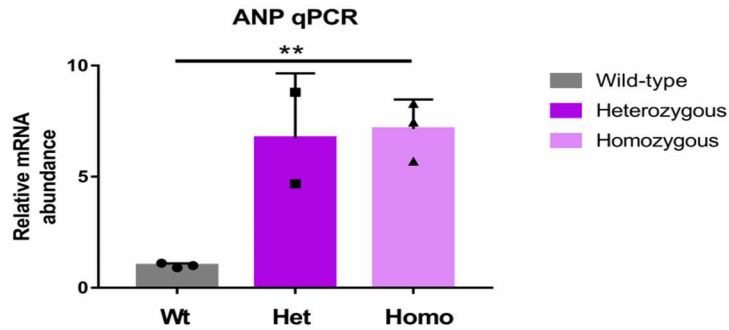
**Figure 7. Qualification of Growth Promoting Signaling Pathways:**

Western blot analysis of phosphorylated AKT (pAKT), phosphorylated ERK (pERK) and MYPT1/2 for wild-type (Wt), heterozygous (Het), and homozygous (Homo) mice for MYTP2 knockout mice.

### **3.6 Quantification of Hypertrophic Molecular Markers by qPCR**

Since hypertrophic molecular markers such as brain natriuretic peptide (BNP) and  $\beta$ -MHC were significantly increased in mice overexpressing MYPT2 in cardiac myocytes (14), we expected to see the opposite trend in MYPT2 knockout mice. We used quantitative PCR (qPCR) to measure the mRNA expression levels of three hypertrophic molecular markers: atrial natriuretic peptide (ANP), BNP, and  $\beta$ -MHC. We found that the transcriptional levels of ANP were significantly increased (Figure 7A); the BNP data was not consistent (data not shown); and the transcriptional levels of  $\beta$ -MHC were significantly decreased (Figure 7B). Taken together, our results suggest a link between cardiac growth and MYPT2 levels; however, the signaling pathways involved remain unknown.

A



B

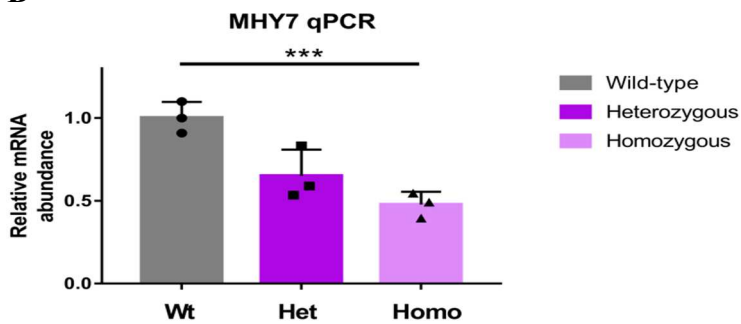


**Figure 7. Alterations in Hypertrophic Molecular Markers:** (A) Quantitative polymerase chain reaction (qPCR) was performed to measure the expression levels of ANP and (B)  $\beta$ -MHC. The cDNA used to determine expression levels was reverse-transcribed from mRNA isolated from 24-week old mice heart tissue.

Results are currently being prepared for submission for publication of the material. Pilz, Renate; Hu, Tingfei; and Casteel, Darren. The thesis author will be co-author of this material.

## Discussion

Cardiovascular health is important as cardiac disease is the first leading cause of death in the United States (17). Researchers have genetically manipulated numerous components of the cardiac contractile machinery to better understand their effects on cardiovascular health. These manipulations include: knocking out or overexpressing MLC kinase 3 (18,19), mutating the MLC phosphorylation sites to non-phosphorylatable alanine (20), and overexpressing MYPT2 (14). However, no previous studies have knocked out MYPT2 and examined its phenotypic effect or studied the signaling pathways altered by the knockout. Therefore, there is a need to study the morphological effects of knocking out MYPT2 and determine the molecular basis underlying these effects.

The main findings of this study are: (i) MYPT2 knockout results in decreased heart size and mass; (ii) MYPT2 knockout mice exhibit increased fractional shortening; (iii) MYPT2 knockout demonstrated increased in ANP and decreased in  $\beta$ -MHC expression. These three major findings are mostly consistent with the results observed in mice with overexpression of MYPT2 (14). However, we did observe some unexpected findings. Previously, Mizutani et al. showed that overexpression of MYPT2 led to an increased expression of BNP. While we were unable to consistently measure BNP transcript levels by qPCR, we did observe an upregulation of ANP, typically seen to increase in parallel with BNP (21). Based on the results of Mizutani, we would have expected ANP levels to decrease in the absence of MYPT2. Therefore, further studies are required to investigate the discrepancies between the two studies.

To find signaling pathways that may explain the observed diminished cardiac size for MYPT2 knockout mice, we examined two growth promoting pathways: the AKT and ERK pathways. The AKT pathway is known to play a role in non-pathological cardiac hypertrophy,

which is seen during normal growth and in athletes (22,23). We expected to detect a downregulation of the AKT growth promoting pathway for the smaller hearts of MYPT2 knockout mice. However, the levels of phospho-serine 473 AKT was unchanged. ERK activation is essential in promoting cell cycle progression and plays a role in inducing cardiac hypertrophy (16,24). Like AKT, the levels of phospho-ERK also remained unaffected in MYPT2 knockout mice. Therefore, the signaling pathways regulated by MYPT2 that lead to smaller heart sizes in the knockout mice remain unknown. Future mRNA sequencing and phosphoproteomic experiments should provide information on the pathways involved.

In summary, MYPT2 knockout mice exhibit diminished cardiac size and increased in fractional shortening, which are related to the alteration in the expressions of ANP and  $\beta$ -MHC.

## REFERENCES

1. Sweeney, H. L., and Hammers, D. W. (2018) Muscle Contraction. Cold Spring Harb Perspect Biol 10
2. England, J., and Loughna, S. (2013) Heavy and light roles: myosin in the morphogenesis of the heart. Cell Mol Life Sci 70, 1221-1239
3. Grassie, M. E., Moffat, L. D., Walsh, M. P., and MacDonald, J. A. (2011) The myosin phosphatase targeting protein (MYPT) family: a regulated mechanism for achieving substrate specificity of the catalytic subunit of protein phosphatase type 1delta. Arch Biochem Biophys 510, 147-159
4. Kampourakis, T., and Irving, M. (2015) Phosphorylation of myosin regulatory light chain controls myosin head conformation in cardiac muscle. J Mol Cell Cardiol 85, 199-206
5. Hartshorne, D. J. (1998) Myosin phosphatase: subunits and interactions. Acta Physiol Scand 164, 483-493
6. Chang, A. N., Kamm, K. E., and Stull, J. T. (2016) Role of myosin light chain phosphatase in cardiac physiology and pathophysiology. J Mol Cell Cardiol 101, 35-43
7. Ichikawa, K., Hirano, K., Ito, M., Tanaka, J., Nakano, T., and Hartshorne, D. J. (1996) Interactions and properties of smooth muscle myosin phosphatase. Biochemistry 35, 6313-6320
8. Hirano, K., Phan, B. C., and Hartshorne, D. J. (1997) Interactions of the subunits of smooth muscle myosin phosphatase. J Biol Chem 272, 3683-3688
9. Feng, J., Ito, M., Ichikawa, K., Isaka, N., Nishikawa, M., Hartshorne, D. J., and Nakano, T. (1999) Inhibitory phosphorylation site for Rho-associated kinase on smooth muscle myosin phosphatase. J Biol Chem 274, 37385-37390
10. Borman, M. A., MacDonald, J. A., Muranyi, A., Hartshorne, D. J., and Haystead, T. A. (2002) Smooth muscle myosin phosphatase-associated kinase induces Ca<sup>2+</sup> sensitization via myosin phosphatase inhibition. J Biol Chem 277, 23441-23446
11. MacDonald, J. A., Borman, M. A., Muranyi, A., Somlyo, A. V., Hartshorne, D. J., and Haystead, T. A. (2001) Identification of the endogenous smooth muscle myosin phosphatase-associated kinase. Proc Natl Acad Sci U S A 98, 2419-2424
12. Muranyi, A., MacDonald, J. A., Deng, J. T., Wilson, D. P., Haystead, T. A., Walsh, M. P., Erdodi, F., Kiss, E., Wu, Y., and Hartshorne, D. J. (2002) Phosphorylation of the myosin phosphatase target subunit by integrin-linked kinase. Biochem J 366, 211-216
13. Terrak, M., Kerff, F., Langsetmo, K., Tao, T., and Dominguez, R. (2004) Structural basis of protein phosphatase 1 regulation. Nature 429, 780-784

14. Mizutani, H., Okamoto, R., Moriki, N., Konishi, K., Taniguchi, M., Fujita, S., Dohi, K., Onishi, K., Suzuki, N., Satoh, S., Makino, N., Itoh, T., Hartshorne, D. J., and Ito, M. (2010) Overexpression of myosin phosphatase reduces Ca<sup>2+</sup> sensitivity of contraction and impairs cardiac function. *Circ J* 74, 120-128
15. Okamoto, R., Ito, M., Suzuki, N., Kongo, M., Moriki, N., Saito, H., Tsumura, H., Imanaka-Yoshida, K., Kimura, K., Mizoguchi, A., Hartshorne, D. J., and Nakano, T. (2005) The targeted disruption of the MYPT1 gene results in embryonic lethality. *Transgenic Res* 14, 337-340
16. Nakamura, Y., Kita, S., Tanaka, Y., Fukuda, S., Obata, Y., Okita, T., Kawachi, Y., Tsugawa-Shimizu, Y., Fujishima, Y., Nishizawa, H., Miyagawa, S., Sawa, Y., Sehara-Fujisawa, A., Maeda, N., and Shimomura, I. (2020) A disintegrin and metalloproteinase 12 prevents heart failure by regulating cardiac hypertrophy and fibrosis. *Am J Physiol Heart Circ Physiol* 318, H238-H251
17. Murphy, S. L., Xu, J., Kochanek, K. D., and Arias, E. (2018) Mortality in the United States, 2017. *NCHS Data Brief*, 1-8
18. Chang, A. N., Battiprolu, P. K., Cowley, P. M., Chen, G., Gerard, R. D., Pinto, J. R., Hill, J. A., Baker, A. J., Kamm, K. E., and Stull, J. T. (2015) Constitutive phosphorylation of cardiac myosin regulatory light chain in vivo. *J Biol Chem* 290, 10703-10716
19. Huang, J., Shelton, J. M., Richardson, J. A., Kamm, K. E., and Stull, J. T. (2008) Myosin regulatory light chain phosphorylation attenuates cardiac hypertrophy. *J Biol Chem* 283, 19748-19756
20. Sheikh, F., Ouyang, K., Campbell, S. G., Lyon, R. C., Chuang, J., Fitzsimons, D., Tangney, J., Hidalgo, C. G., Chung, C. S., Cheng, H., Dalton, N. D., Gu, Y., Kasahara, H., Ghassemian, M., Omens, J. H., Peterson, K. L., Granzier, H. L., Moss, R. L., McCulloch, A. D., and Chen, J. (2012) Mouse and computational models link Mlc2v dephosphorylation to altered myosin kinetics in early cardiac disease. *J Clin Invest* 122, 1209-1221
21. Hofmann, F. (2018) A concise discussion of the regulatory role of cGMP kinase I in cardiac physiology and pathology. *Basic Res Cardiol* 113, 31
22. Walsh, K. (2006) Akt signaling and growth of the heart. *Circulation* 113, 2032-2034
23. DeBosch, B., Treskov, I., Lupu, T. S., Weinheimer, C., Kovacs, A., Courtois, M., and Muslin, A. J. (2006) Akt1 is required for physiological cardiac growth. *Circulation* 113, 2097-2104
24. Ramos, J. W. (2008) The regulation of extracellular signal-regulated kinase (ERK) in mammalian cells. *Int J Biochem Cell Biol* 40, 2707-2719